Remote Sensing of Environment 218 (2018) 32–43

Contents lists available at ScienceDirect

Remote Sensing of Environment

journal homepage: www.elsevier.com/locate/rse

A tree-based approach to biomass estimation from remote sensing data in a tropical agricultural landscape

Sarah J. Graves[a,b,*], T. Trevor Caughlin[a,c], Gregory P. Asner[d], Stephanie A. Bohlman[a,e]

[a] School of Forest Resources and Conservation, University of Florida, Gainesville, FL 32611, United States of America
[b] Nelson Institute for Environmental Studies, University of Wisconsin-Madison, Madison, WI 53706, United States of America
[c] Department of Biological Sciences, Boise State University, Boise, ID 83725, United States of America
[d] Department of Global Ecology, Carnegie Institution for Science, Stanford, CA 94305, United States of America
[e] Smithsonian Tropical Research Institute, Apartado 0843–03092, Balboa, Ancon, Panama

ARTICLE INFO

Keywords:
LiDAR
Silvopasture
Land-sharing
Panama
Trees outside forests
Trees on farms
Agroforestry
Agricultural carbon
Allometric model
Tropical trees

ABSTRACT

Agricultural land now exceeds forests as the dominant global biome. Because of their global dominance, and potential expansion or loss, methods to estimate biomass and carbon in agricultural areas are necessary for monitoring global terrestrial carbon stocks and predicting carbon dynamics. Agricultural areas in the tropics have substantial tree cover and associated above ground biomass (AGB) and carbon. Active remote sensing data, such as airborne LiDAR (light detection and ranging), can provide accurate estimates of biomass stocks, but common plot-based methods may not be suitable for agricultural areas with dispersed and heterogeneous tree cover. The objectives of this research are to quantify AGB of a tropical agricultural landscape using a tree-based method that directly incorporates the size of individual trees, and to understand how landscape estimates of AGB from a tree-based method compare to estimates from a plot-based method. We use high-resolution (1.12 m) airborne LiDAR data collected on a 9280-ha region of the Azuero Peninsula of Panama. We model individual tree AGB with canopy dimensions from the LiDAR data. We apply the model to individual tree crown polygons and aggregate AGB estimates to compare with previously developed plot-based estimates. We find that agricultural trees are a distinct and dominant part of our study site. The tree-based approach estimates greater AGB in pixels with low forest cover than the plot-based approach, resulting a 2-fold difference in landscape AGB estimates between the methods for non-forested areas. Additionally, one third of the total landscape AGB exists in areas having < 10% cover, based on a global tree cover product. Our study supports the continued use and development of allometric models to predict individual tree biomass from LiDAR-derived canopy dimensions and demonstrates the potential for spatial information from high-resolution data, such as relative isolation of canopies, to improve allometric models.

1. Introduction

At 38% of Earth's surface area, cropland and pasture exceeds forest as the dominant global terrestrial biome (FAO, 2016). A common pathway from forest to agriculture, especially prevalent in tropical areas, is conversion of forest to pasture land, followed by conversion to croplands (Graesser et al., 2015). Globally, an estimated 83 million hectares of primary and degraded tropical forest have been converted to agricultural land between the 1980s and 1990s (Gibbs et al., 2010). These large shifts from forest area to cropland are associated with a loss of carbon storage and sequestration because of the reduction of standing biomass and soil carbon (Pan et al., 2011).

Despite the global decline of forest cover, agricultural areas in the tropics are characterized by remnant trees that provide ecosystem services, including seed sources for forest recovery, habitat for wildlife, and valuable forest products for landowners (Harvey et al., 2005, 2006; Harvey and Haber, 1999; León and Harvey, 2006; Medina et al., 2007; Prevedello et al., 2017; Slocum and Horvitz, 2000; Zahawi et al., 2013). Agricultural tree cover can exist as individual trees, scattered groups of trees, live fences, windbreaks, and small forest fragments or riparian forests (Griscom et al., 2011; Harvey et al., 2006; Plieninger, 2012). In addition, while tropical agricultural lands contain less standing biomass than forests, agricultural trees are important sinks and pools of carbon in the form of living biomass (Zomer et al., 2016). The dominance of agricultural land means that tropical agricultural areas have an influential role in global carbon dynamics with potential for additional

* Corresponding author at: Nelson Institute for Environmental Studies, University of Wisconsin-Madison, Madison, WI 53706, United States of America.
E-mail address: sjgraves@wisc.edu (S.J. Graves).

https://doi.org/10.1016/j.rse.2018.09.009
Received 30 November 2017; Received in revised form 26 July 2018; Accepted 13 September 2018

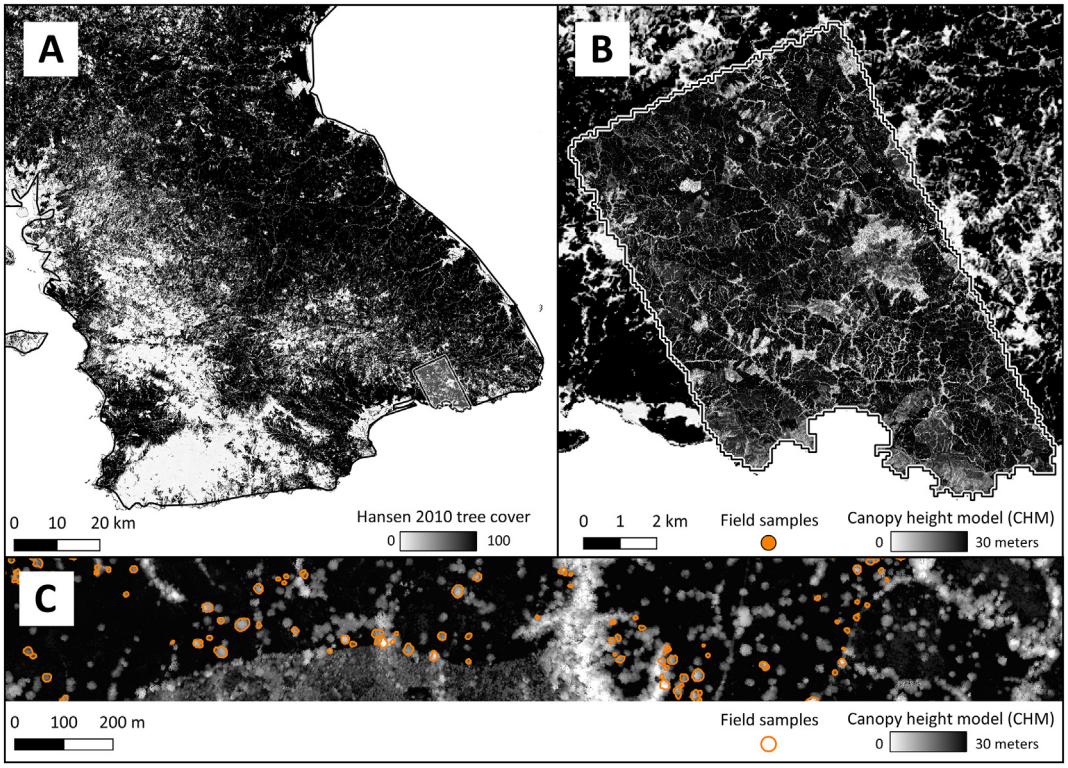

Fig. 1. Map of the study site on the Azuero Peninsula of Panama. A) Tree cover on the Azuero Peninsula from the 2010 Hansen global tree cover analysis (Hansen et al., 2013). B) Carnegie Airborne Observatory (CAO) canopy height model (CHM) from 2012 of the 9280-hectare study site. Orange dots show the locations of the field data. The global tree cover product is shown outside the study site. C) Subset of study site showing mapped crown polygons on the CHM.

emissions through the loss of existing agricultural tree biomass (Harvey et al., 2011), or enhanced sequestration through forest and landscape restoration (Chazdon et al., 2016b).

Remotely sensed data are increasingly used to estimate forest cover and carbon stocks from local to global scales. Landcover classification into discrete categories by optical satellite data, such as the Landsat and MODIS systems, has contributed to an understanding of dynamics between forest and agricultural areas in Latin America (Aide et al., 2013; Graesser et al., 2015). Given the large difference in biomass and carbon between forest and agricultural areas, these land cover classifications provide critical information for quantifying biomass and carbon dynamics. However, variation in biomass within forest and agricultural areas can be substantial, and the boundary between what is forest and not forest imprecise. As a result, continuous measurements of vegetation structure, such as percent tree cover and tree height, are critical for understanding forest dynamics in heterogeneous landscapes, and indirect estimation of vegetation structure from optical sensors remains an important challenge (Caughlin et al., 2016; Hansen et al., 2013).

Active remote sensing technologies, such as light detection and ranging (LiDAR), can provide structural information to further resolve variation in canopy cover and aide in biomass estimation. For example, LiDAR measurements of the canopy surface height (at 0.1 to 1 ha spatial resolution), when matched to field-measured tree inventory plots where biomass has been estimated, can be used to refine estimates of AGB from optical image data to provide country-wide estimates of biomass or carbon density (Asner et al., 2013, 2016; Asner and Mascaro, 2014). One primary benefit of this approach is that field-calibrated models of plot biomass can be applied to large areas to provide spatial data on the variation in a property of interest.

However, methods that combine inventory plots with remote sensing data at the plot scale (0.1 to 1 ha) may perform poorly in tropical agricultural areas. This is because the vegetation structure of agricultural areas is different than that of forests. Agricultural areas contain large areas with few or no trees, so plot sampling approaches typically used in forest studies do not measure agricultural tree structure well. To accurately quantify the contribution of agricultural trees to landscape AGB requires remote sensing methods that can represent individual trees, rather than the height of a smoothed canopy surface. With advent of high spatial resolution LiDAR data, and algorithms to detect individual trees (Coomes et al., 2017; Dalponte et al., 2015; Duncanson et al., 2014; Ferraz et al., 2016; Zhen et al., 2016), more tree-centered AGB estimates are possible, where the size of individual trees, rather than the height or canopy cover of forest plots, is measured from remote sensing data and linked to field observations of those same individuals.

Studies comparing plot- and tree-based approaches to estimate AGB in ecosystems with heterogeneous tree cover highlight the importance of measuring individual trees. In an African savanna, Colgan et al. (2013) found that a plot-based method underestimated AGB because the plot-level top of canopy height measurement could not distinguish between differences in plot structure, such as a homogeneous canopy of small trees versus a heterogeneous canopy of one or a few large trees. Additionally, Coomes et al. (2017) implemented a tree-based approach to estimate biomass in closed canopy tropical forest in Malaysia. The authors argue that while the tree-based approach had slightly higher uncertainty than the plot-based approach, the continued development of these methods is needed to provide input to models of individual tree dynamics and fine-scale forest biomass, which may be hard to resolve with plot-based data and analysis. Finally, the utility of using individual tree crown size metrics to quantify biomass and carbon stocks with LiDAR data was recently demonstrated with a global dataset across forest types (Jucker et al., 2016), paving the way for application of these methods in different ecosystems and landscapes.

In this study, we implement a tree-based method for estimating AGB of an agricultural landscape in Panama, and compare our tree-based estimates with plot-based estimates for the same area. The objective of this study is to assess a tree-based versus a plot-based approach to estimate AGB of agricultural landscapes, with respect to the agricultural tree cover contribution to landscape AGB, model error, and the

scalability to large areas for landscape assessments. We hypothesize that tree-based approaches can provide large improvements in AGB estimation because they capture the high structural heterogeneity in agricultural landscapes with dispersed tree cover, and because this dispersed tree cover is not directly measured in plot-based estimates. This study addresses two questions; First, what is the contribution of trees in agricultural areas to landscape estimates of AGB? Second, how do individual tree- and plot- based approaches to AGB estimation differ?

2. Methods

2.1. Study site

The Azuero Peninsula of Panama has a long history of agricultural development, which has left a landscape dominated by crop fields and pastures (Heckadon Moreno, 2009; Metzel and Montagnini, 2014). The 8000 km^2 peninsula is located on the Pacific side of Panama at approximately 7.5° N, and 80.5° W (Fig. 1A). Though the peninsula is now dominated by non-forest land use, the area was historically covered in tropical dry broadleaf forest to the south and east, and moist broadleaf forest in the west based on temperature, precipitation, and species distribution patterns (Olson et al., 2001). In the most southern region of the peninsula where this study was conducted, mean annual rainfall is 1946 (standard deviation = 65) mm per year with on average 5.2 months of drought characterized by < 100 mm of rainfall per month (Park et al., 2010). The current scarcity of forest on the Azuero Peninsula is a result of centuries of forest clearing for cattle and farming, initiated by Spanish colonists and intensified during the latter half of the 20th Century (Heckadon Moreno, 2009). The study site for this research is 9280 ha area in the southernmost region of the Azuero Peninsula (Fig. 1B) and is dominated by cattle pastures on hills with steep slopes.

2.2. Field and remote sensing data

In January 2012, the Carnegie Airborne Observatory (CAO) collected hyperspectral and LiDAR data using the AToMS system (Asner et al., 2012). The discrete point-cloud LiDAR returns were processed to a ground surface image (last return) and a maximum height image (first return), from which a canopy height model (CHM) was derived. The CHM had a spatial resolution of 1.12 m and represents the height of surface features, such as trees.

In May–July of 2012 and 2013, a sample of trees on private lands was located and marked in CAO high-resolution (1.12 m) georeferenced visible-near infrared images using a tablet computer equipped with a GPS (Xplore Technologies; Austin, TX) and GIS software (ESRI Arc GIS 10.0; Redlands CA). All trees were located within the area of the study site covered by the airborne data and concentrated in the southern and northeastern region (Fig. 1C). Trees were selected to provide a representative sample of the species and sizes of trees in pastures found on the landscape. For each tree, we recorded the species, height, diameter at breast height (measured at 1.3 m), and whether it was in a pasture or forest. Maximum tree height was measured with a laser altimeter (Nikon Forestry 550, Nikon Corporation; Tokyo, Japan). Crown boundaries were digitized in the field directly onto the digital image (Fig. 2). Later in the lab, tree crown boundaries were adjusted and refined using the LiDAR CHM in ENVI (Exelis Visual Information Solutions; Boulder, Colorado). A total of 1059 individual trees across 43 species were included in our dataset (Graves et al., 2016).

2.3. Methods workflow

The workflow consisted of five steps (Fig. 2). Steps one through three (Sections 2.4–2.6) generated a model to estimate individual tree AGB from LiDAR data and a landscape map of forest cover based on coverage of individual tree crowns. Steps four and five (Sections 2.7–2.8) scaled tree-based AGB to the landscape and compared the AGB-tree estimates (this study) and AGB-plot estimates (Asner et al., 2013) along a forest cover gradient produced with LiDAR data (this study) and a global tree cover product (Hansen et al., 2013). The steps are explained in more detail in the following sections.

2.4. Development of field-based allometric AGB model

First, we calculated field-based AGB (AGB-Chave) with the Chave et al. (2005) pantropical equation for dry forests where AGB-Chave was the estimated biomass (kg), tree diameter was the diameter of stems measured at breast height (cm), tree height (m) was the maximum height of the canopy, and wood density was the taxon-specific wood density (g/cm^3). Diameter and tree height were provided from field measurements. Wood density was provided from the Neotropical wood density database (Chave et al., 2006). Of the 43 species included in this study, 37 (92%) had wood density values in the Neotropical database. For the remaining six species, genus or family level wood density average were used. Trees with multiple stems were common, with 30% of trees having more than a single stem. For trees with multiple stems, we applied the Chave allometric model to each stem, and summed the stem-level AGB to generate a whole tree estimate of AGB (Chave et al., 2008).

Though we were not able to directly measure AGB by felling and weighing individual trees, the Chave et al. (2005) allometric models have been widely used for estimating AGB across the tropics (e.g. Baccini et al., 2012; Girardin et al., 2010). Additionally, the allometric models provided a good approximation of AGB of dispersed tree cover in a South African savanna (Colgan et al., 2013), and an agricultural landscape in Western Kenya (Kuyah et al., 2012). The Chave et al. (2005) models were also used in the plot-based AGB estimation approach used in the national analysis of aboveground carbon stocks in Panama (Asner et al., 2013), to which our AGB estimates were compared. To make direct comparisons to the plot-based method, we did not use the revised tropical allometric models (Chave et al., 2014).

2.5. Development of AGB-LiDAR model

Second, using AGB-Chave as our observed AGB, we developed a predictive AGB allometric model based on LiDAR-derived measurements of crown size, maximum crown height, and a metric for the relative isolation of each tree (Fig. 2). Crown size was determined from the manually digitized tree crowns for all field-measured trees. We calculated crown diameter from the polygon crown area. Maximum tree height was measured from the CHM. There was a strong correlation between the field and the LiDAR measured height (Pearson's correlation coefficient = 0.81) with no apparent systematic bias (Supplementary material, Section S1). Following the approach of Jucker et al. (2016), we calculated a composite metric of crown size by multiplying maximum crown height by crown diameter (HCD). This method was attractive because it combined two measurements into a single covariate, thus avoiding issues of collinearity between crown size and height.

Motivated by field-observed differences in diameter, height, and crown size between trees in closed canopy forests versus open canopy pastures, we classified our field sampled trees into three groups based on the amount of crown edge they share with other crowns. The three groups were: isolated trees with no edge shared with another crown; forest trees with complete sharing of crown edge; and intermediate trees with anywhere between 1 and 99% of the crown edge shared with another crown. The shared edge was quantified by measuring the percentage of the polygon perimeter touching another polygon.

Because our samples had an uneven size distribution, we used a binning approach to develop a linear model to predict AGB (Duncanson et al., 2015; Jucker et al., 2016). We compare the binned model to ordinary least squares regression (OLS) in the Supplementary material,

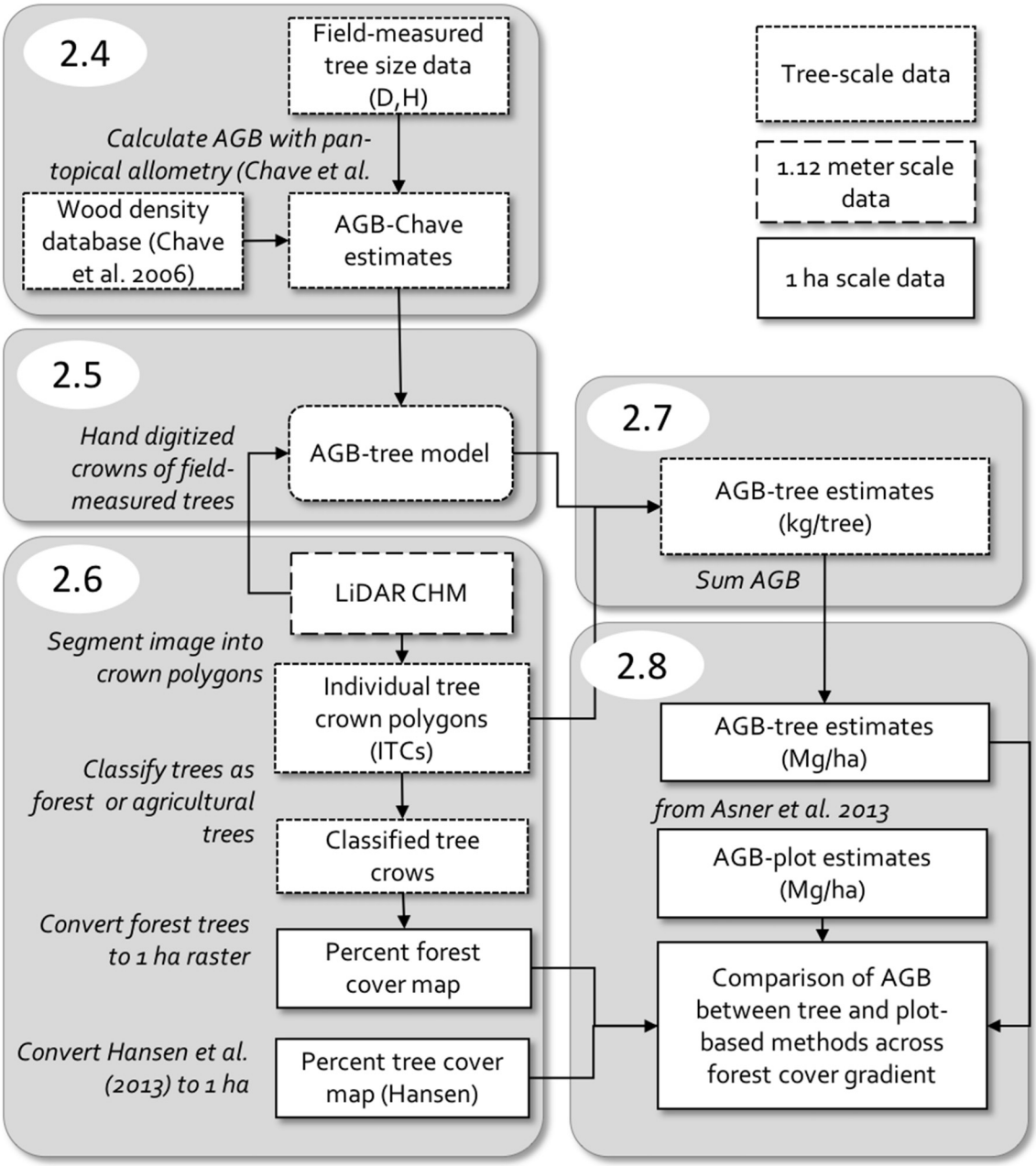

Fig. 2. Methods workflow of this study to produce above ground biomass (AGB) estimates from field data and a LiDAR canopy height model (CHM). White boxes represent data products (square corners) or models (rounded corners) and outline patterns indicates the spatial scale of the data or model. Numbers in each grey box correspond to sections in the text.

Section S2. For each tree group (isolated, intermediate, or forest), we split the data into equally sized bins based on the logarithm of AGB. A leave-one-out cross validation approach (LOOCV) was used to evaluate the fit of the model, where all but one observation was held out of model development and used for evaluation, and the number of iterations was equal to the number of samples in the dataset (n = 1059). For the data used for model development, the mean HCD and AGB were calculated from the observations within each bin. The mean HCD and AGB were then log-transformed to ensure normality, and a linear model was fit with log transformed HCD as a predictor variable and log-transformed AGB as a response variable:

$$\ln(\mathrm{AGB}) = \beta_0 + \beta_1 \ln(\mathrm{HCD}) + \beta_3 \mathrm{Group} \quad (1)$$

Model predictions were corrected with the Baskerville Correction (Baskerville, 1972), which was necessary for the linear model with log-log transformation of the data. Model fit was assessed on the model predictions of back transformed AGB (in kg units) for the out of sample un-binned data. We calculated the coefficient of determination (R^2), root mean squared error in kg (RMSE), and percent bias for the out-of-sample predictions. To estimate the uncertainty of AGB-tree estimates across the landscape, we also estimated model parameters for 200 random samples of 90% the field data. We then calculated the mean and 95% confidence intervals of landscape AGB-tree estimates based on the 200 models (Supplementary material, Section S2).

2.6. Landscape map of agricultural and Forest tree crowns

Third, we segmented the LiDAR CHM into individual tree crown polygons (ITCs) across the entire landscape and extracted the maximum height and crown diameter (crown diameter = 2 ∗ sqrt(crown area/pi))

of each ITC (Fig. 2). To do this, we applied the image segmentation function of the SAGA GIS program (http://www.saga-gis.org/en/) to the 1.12 m CHM of the study site. This segmentation produced nearly 500,000 individual polygons representing ITCs. With the SAGA approach, unlike other segmentation algorithms (i.e. itcSegment, Coomes et al., 2017), there are no overlapping crowns, which facilitates calculation of the amount of shared edge between polygons.

The SAGA segmentation produced crowns that were on average larger than the crowns we manually delineated. We reduced the crown diameter of the automatically segmented polygons by 25% to meet the crown diameter and AGB values of the field crowns. The correlation between the manually and automatically segmented crowns (after the reduction in crown diameter) for HCD and AGB differs among the three tree groups, and is highest for the isolated trees. Details about how the automatic segmentation compares to the manually delineated field crowns are provided in the Supplementary material, Section S3. We applied our LiDAR model to all ITCs using the reduced crown diameter values.

The objective of this study was to quantify the amount of AGB that occurs outside of forests. Therefore, we needed a forest cover classification to identify areas that are forest and non-forest. We did this in two ways; one by using a global dataset of tree cover (Hansen et al., 2013), and two by creating a forest cover classification directly from the ITC polygons generated from the LiDAR data. For the Azuero landscape, forested trees could be distinguished from non-forest trees (trees in pastures or part of live fences) based on the amount of crown edge they shared with another crown. In the same manner that we grouped trees into 3 classes (isolated, intermediate, and forest), we split all ITCs into two groups based on the calculated amount of shared edge. ITCs with $< 65\%$ of their edge touching another ITC were classified as agricultural trees because they were relatively isolated from other trees. ITCs with $\geq 65\%$ of their crown edge touching another ITC were classified as forest trees. The 65% threshold was determined iteratively until the threshold produced by a data-based categorization matched our field observations. The discrete classification of ITCs into forest and non-forest groups allowed us to sum the crown area of only our forested crowns when aggregating data to the 1-ha scale. We note that with the 65% threshold, ITCs located along the edge of forest patches and riparian forests were often classified as agricultural trees; an appropriate classification as these trees experience microclimate conditions similar to trees growing in small tree clumps in pastures due to the large amount of edge (Laurance et al., 2002). The crown classification was performed in R, using a polygon coverage layer generated in ArcGIS.

The classified ITCs were used to generate a map of forest cover at 1 ha resolution. Individual tree crown polygons were assigned to a 1 ha pixel based on their center point. The amount of forest tree crown cover for each 1-ha pixel was determined by summing the ITC area for all forest ITC center points that fell within each pixel. The per-pixel summed forest tree crown area was then divided by the pixel size (1 ha) to determine the percent cover of forest tree crowns (Fig. 3 A & B). The percent forest tree cover metric, or forest cover for simplicity, represents the proportion of ground area composed of tree cover that is part of a continuous canopy of trees. The proportion of the pixel not covered by forest trees is either non-tree cover, such as grass, water, or developed structures, or trees that are not part of a continuous forest, such as isolated trees in pastures (those with $< 65\%$ shared edge). A comparison of the LiDAR forest cover, the LIDAR tree cover (which includes all forest and non-forest trees), and an independent global dataset of tree cover from Hansen et al. (2013) is shown in the supplementary material, Section S4. A subset of the study site highlights how the Azuero forest cover and global tree cover datasets capture areas of dense tree crowns, but show little cover in areas with dispersed tree crowns (Fig. 3).

2.7. Landscape AGB estimation from tree-based LiDAR model

Fourth, by applying the AGB-tree model (from Section 2.5) to the classified ITCs (from Section 2.6), we generated an estimate of AGB from our tree-based method (AGB-tree estimates, Fig. 2). The AGB LiDAR model was applied to 449,965 ITCs across the entire 9280 ha study site. This produced a dataset of estimated AGB (in kg) from the AGB LiDAR model for all ITCs. The AGB estimates of all ITCs were summed in a 1 ha grid, producing an estimate of AGB density in Mg AGB per hectare (AGB-tree estimate) that was compared to a published plot-based estimate of AGB (AGB-plot estimate) for the same study site (Asner et al., 2013).

2.8. Calculation of the difference between tree- and plot-based AGB estimates

Fifth, the AGB-tree estimate was directly compared to the AGB-plot estimate from Asner et al. (2013) across a gradient of forest cover (Fig. 2). Asner et al. (2013) used the same LiDAR data used in our current study to estimate aboveground carbon density (ACD) for all of Panama, which we converted to AGB (AGB = ACD/0.48). Rather than estimating AGB of individual trees from the aerial images as in our current study, Asner et al. (2013) used a LiDAR metric of Top of Canopy Height (TCH), derived for 1-ha pixels to estimate AGB. The study used 228 field inventory plots throughout Panama where all tree stems ≥ 10 cm DBH were measured. The DBH of all trees in each field plot was converted to AGB using the same allometric equations used in our current study (Chave et al., 2005) and summed to generate a plot-level AGB. An equation to predict the plot-level, field-based AGB estimate from the LiDAR-based TCH metric was developed. The equation was applied to the TCH value of all 1-ha pixels across the study site to produce landscape estimates of AGB in Mg/ha (AGB-plot estimates).

3. Results

3.1. Estimation of AGB from crown attributes

For the 1059 field-measured trees, stem diameter (for the 313 trees with multiple stems, the diameter of the largest diameter was used) had a non-linear relationship with height and crown diameter (Fig. 4 A, B). Variation in these relationships could be seen between the three groups of trees with different amounts of shared crown edge (isolated, intermediate, and forest), especially in the stem diameter and height relationships. Forest trees (complete shared edge) were taller with smaller crowns than isolated trees (no shared crown edge) for a given DBH. The tree HCD, the canopy size metric (height times crown diameter) used to relate image crown measurements to field-based allometric predictions, showed a nearly linear relationship with AGB on a log scale (Fig. 4 C), as has been seen with a global dataset (Jucker et al., 2016). The linear model of AGB (Fig. 4 D) fit to the three crown edge groups, included the following parameters:

$$\ln(\text{AGB}-\text{LiDAR}) = -3.71 + 2.07 \times \ln(\text{HCD}) - 0.45 \times \text{Intermediate} - 0.50 \times \text{Forest} \quad (2)$$

All parameters in the model were significant (p-value < 0.005). On back-transformed values of AGB in kg, the binned model explained 43% of the variation in AGB, had an out-of-sample RMSE of 1800 (kg), and model bias of 27%. The model showed a deviation from the 1:1 line, with underpredictions of AGB for trees with AGB < 500 kg. To identify if spatial autocorrelation was present in our sample dataset, we examined the spatial patterns of the residuals of the linear model using a semivariogram. We found that the semivariance did not increase with increasing distance between the samples, indicating minimal evidence for spatial autocorrelation in the model residuals.

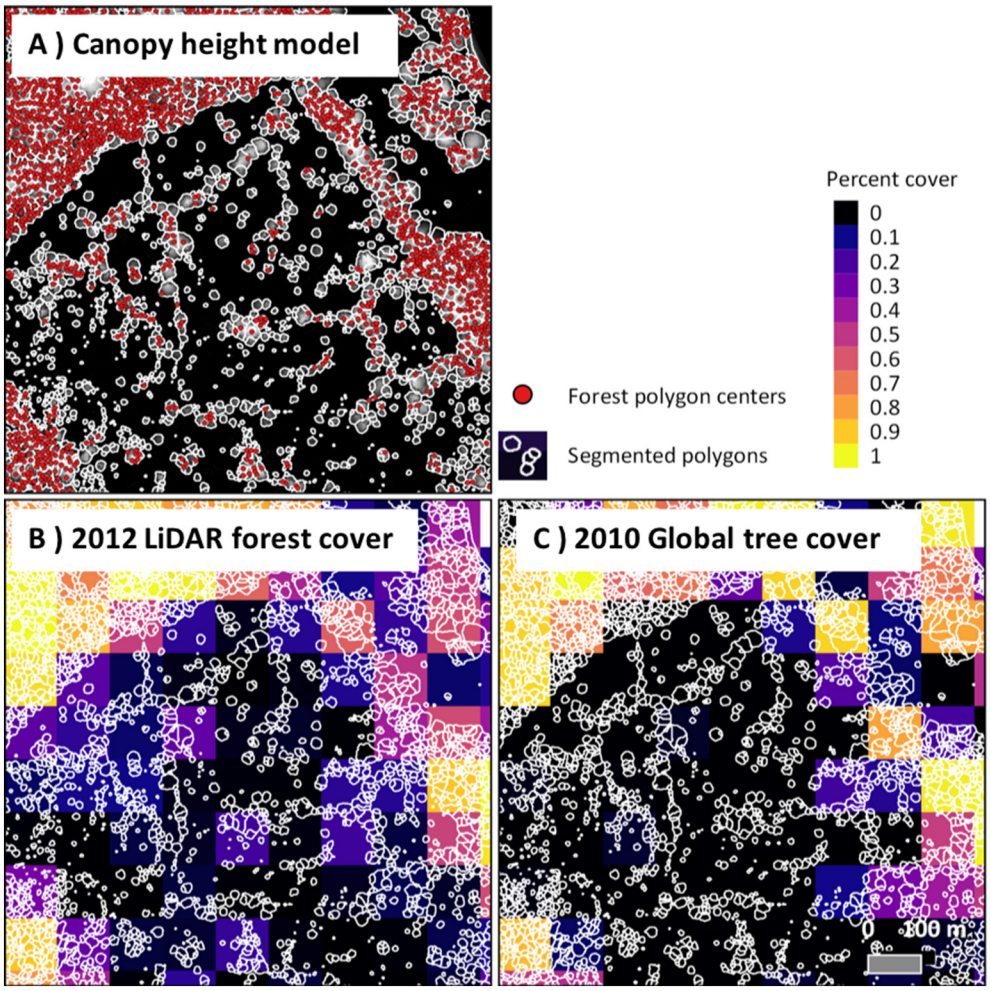

Fig. 3. Subset (100 ha) of the Azuero study area showing heterogeneous tree cover distribution. All panels show the same area with outlines of the segmented tree crown polygons (ITCs) in white. In panel A, forest tree polygons (polygons with > 65% shared edge) are marked with red center points. The background of panel A shows the 2012 LiDAR 1.12 m resolution canopy height model (lighter colors have greater height). Lower panels show 1-ha resolution data of percent forest cover generated with the forest tree polygons (panel B) and percent tree cover circa 2010 from the Hansen global tree cover product (panel C). (For interpretation of the references to color in this figure legend, the reader is referred to the web version of this article.)

3.2. Landscape comparison of tree-based and plot-based AGB estimation

The maximum and mean AGB of the tree and plot-based estimates were similar, at approximately 240 and 26 Mg/ha for the tree-estimates, and 254 and 23 for the plot-estimates (Fig. 5). Distribution of AGB shows that the plot-estimates are more concentrated on the lower end of AGB, whereas the tree-estimates are relatively higher at the intermediate range between 25 and 75 Mg/ha (Fig. 5A). The higher tree-estimates relative to plot-estimates in the 25–75 Mg/ha range are seen in pixel-by-pixel comparisons as well (Fig. 5 B). At high levels of AGB, the plot-estimates are larger than the tree-estimates. This indicates that in areas of high tree cover, which shows a positive relationship with AGB, the plot-based predictions are detecting a greater amount of AGB.

Comparisons of AGB estimates from the tree-based and plot-based methods showed a pattern of higher AGB estimates using the tree-based method at low levels of forest cover (Fig. 6). In both the tree and plot-based methods, AGB per hectare, and the variability in AGB per hectare, increased with the amount of forest cover. The tree-based estimates had an intercept greater than zero, meaning areas with zero forest cover on average had non-zero AGB, which is capturing the AGB of dispersed tree crowns. In contrast, plot-based estimates at zero forest cover were close to zero. The higher AGB-tree estimates continue throughout the range of forest cover, with values becoming more similar at higher forest cover due to the increased AGB-plot estimates at these high levels of cover.

Spatial patterns of AGB followed the broad patterns of forest cover, with the highest and lowest AGB seen in areas of high and low forest cover respectively (Fig. 7). Forested areas, such as patches of secondary forest and riparian forests, are visible both in the tree- and plot-based methods. Outside of these prominent forested areas is pasture land with agricultural trees, where the AGB-tree estimates are higher than the plot-based estimates throughout the study site.

The distribution of the landscape AGB differs between the two methods. We classified the landscape into 10% cover intervals using our forest cover classification from the 2012 LiDAR data. We report our results as the proportion of the total landscape AGB and sum of total landscape AGB in each 10% bin (Fig. 8). Because our focus was to quantify the AGB in of non-forest areas, we limited our results to areas with < 50% cover. The AGB estimates from both the tree and plot-based methods are highest at low levels of forest cover and decline as cover increases. The counterintuitive result that areas with the lowest forest cover have the highest AGB was driven by the dominance of the low forest cover areas on the landscape (Fig. 8 A, C). Areas with < 10% forest cover dominated the landscape at 3396 ha (37%, Supplementary material, Section S4) and made up 25,000 Mg of AGB (10% of the landscape AGB) from the tree-based approach, and 11,000 Mg of AGB (6% of the landscape AGB) from the plot-based approach. The differences between the tree and plot-based approaches were greatest at 10% forest cover, and became more similar with increasing forest cover.

To understand the landscape in terms of a global metric of tree cover, we also summarized the tree- and plot-based estimates of AGB according to a global dataset of tree cover from 2010 (Fig. 8 B, Hansen et al., 2013). Here, the areas with < 10% tree cover make up 4772 ha (52%, Supplementary material, Section S4). Areas having between 0 and 10% tree cover contained 62,000 Mg of AGB (26% of the landscape AGB) with the tree-based estimates, and 37,000 Mg of AGB (18% of the

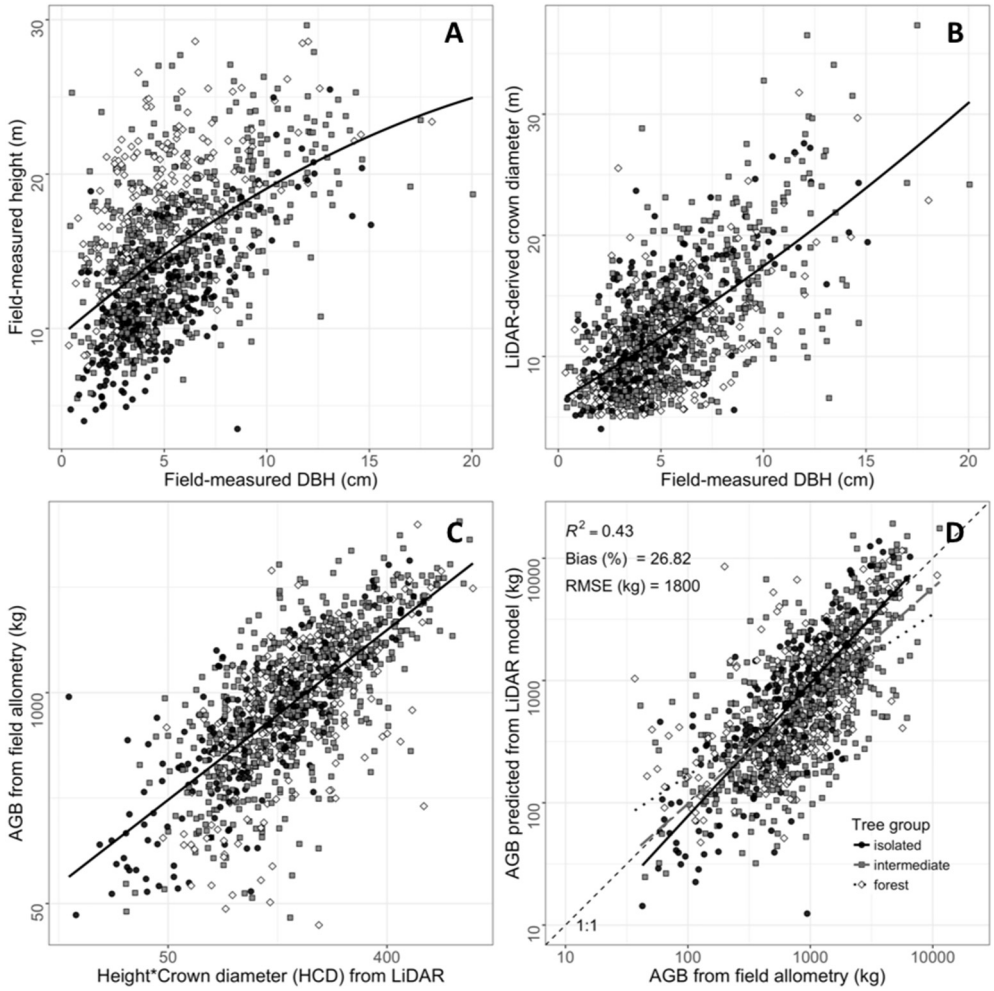

Fig. 4. Size measurements for 1059 field-measured trees. Each point represents an individual. Colors and shape represent the tree group based on location in open to forest conditions. Quadratic models are fit through data in panels A and B (solid blacklines), and linear models are fit though data in panels C (solid black lines) and D (color and line type by tree group). Panel D shows the above ground biomass (AGB) from Chave et al. (2005) allometry and LiDAR model predictions.

AGB) with the plot-based estimates (Fig. 8 B, D). Furthermore, areas with 0% tree cover, which make up 38% of the landscape area, contained 25% and 17% of the landscape AGB with the tree- and plot-based methods, respectively. As with the forest cover classes, the differences between the approaches decreased in the higher cover classes.

4. Discussion

4.1. Improvement of allometric models with airborne LiDAR data

Landscape estimates of above ground biomass (AGB) provide novel data to address ecological questions beyond what ground-based estimates can provide (Colgan and Asner, 2014; Dahlin et al., 2012).

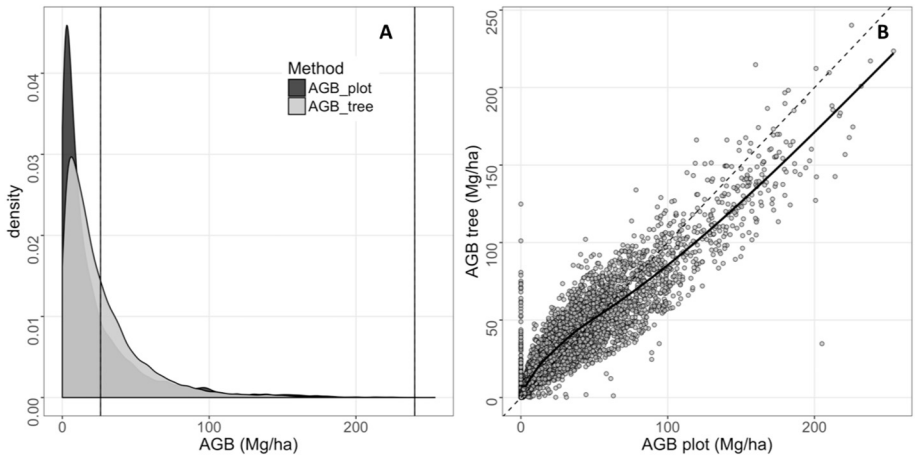

Fig. 5. Distribution of AGB between the tree and plot-based estimates of above ground biomass (AGB). A) Density plot of AGB values where colors indicate the method. Vertical lines are the maximum and mean values for each method (lines overlap). B) Each point representing a 1-ha pixel in the study site. Lines show the 1:1 relationship (dashed) and a general additive model fit to the data (solid).

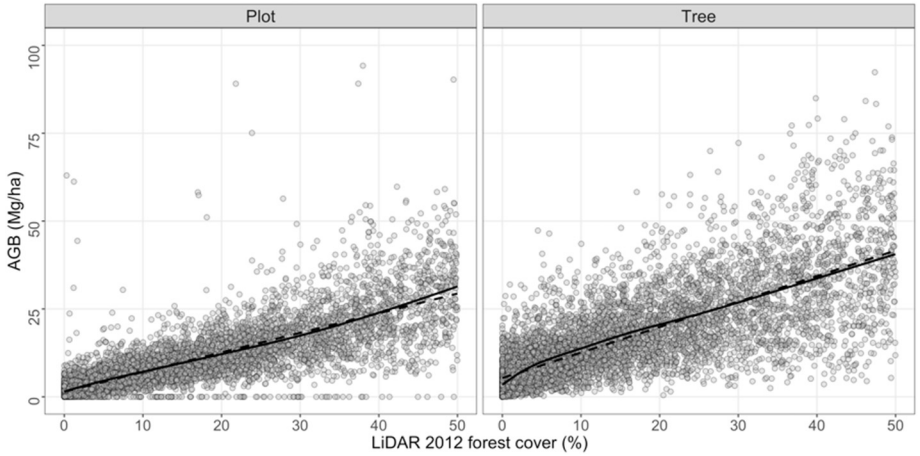

Fig. 6. Estimates of above ground biomass (AGB) for a tree-based (this study) and plot-based (Asner et al., 2013) methods along a gradient of forest cover derived from the 2012 LiDAR data. Each point represents a single 1 ha pixel. Lines represent a generalized additive model with smoothing (solid) or and a linear model fit through the data (dashed).

Airborne LiDAR data, which can provide measurements of individual trees continuously over large areas and from a perspective above the canopy, offers an opportunity to develop allometric models of AGB using remote measurements of vegetation structure (Colgan et al., 2013; Dalponte and Coomes, 2016; Jucker et al., 2016). In our study, we relied on a two-step process that first estimates AGB using widely accepted allometries for tropical trees (Chave et al., 2005), and second develops a statistical model with LiDAR metrics to reproduce those estimates (Jucker et al., 2016).

Our tree-based models were promising for two reasons. First, we support the use of the allometric relationship between a single metric of combining height and crown diameter (HCD) with aboveground biomass (AGB) at a local scale that was applied successfully in a global study of canopy trees (Jucker et al., 2016). Our field dataset was 10% in size of the global dataset and represented a narrower range of crown size and AGB, which led to the local model explaining a lower amount of variation in the data and higher error and bias relative to the global model (Fig. 4). Nonetheless, the simple metric was able to capture the patterns of AGB seen across our study site, and used to quantify the amount of AGB contributed by isolated trees and tree clusters in non-forested agricultural land. We found that a relatively simple OLS model had lower uncertainty than the model that binned trees into size categories, with an RMSE that was 800 kg lower than the binned model (Fig. 4 Supplementary material, Section S1). However, the binned model had much lower bias than the OLS model. This result points to the need to consider tradeoffs between these different model structures when developing landscape-scale predictions of biomass.

Second, we incorporated a metric that captures crown competition by allowing trees to be in one of three groups based on their relative isolation from other trees. By applying the model to the three distinct groups, we were able to model the differences in AGB driven by different height, stem diameter, and crown diameter allometries among trees in different competitive environments (Fig. 4A). For example, for trees with low AGB, forest trees had higher HCD than isolated trees (Fig. 4C). Grouping the trees into these simple categories based on their relative isolation is a simple way to capture the allometric variability in areas of heterogenous tree cover and improve landscape predictions of AGB.

Not only do LiDAR data allow for measurements of many individual trees continuously over large areas, LiDAR also provides innovative variables that help explain variation of tree biomass, such as crown area and isolation. Because these metrics are focused on characteristics of a tree's canopy, they are challenging to measure from the ground, but easily measured for trees in open areas with airborne data that has an above canopy perspective. This supports other work that identifies tree characteristics, such level of light competition and wind susceptibility, as important drivers of allometric relationships that can improve estimates of AGB (Henry and Aarssen, 1999; Holbrook and Putz, 1989; Lines et al., 2012). Our results suggest that a measurement of crown isolation could be widely applied to allometric models to improve biomass estimates, especially in trees found outside forests.

The key element that needs improvement in the workflow for predicting landscape level, tree-based AGB is automatic segmentation of individual tree crowns. For much of our study site which has limited tree canopy cover, individual crown detection from the LiDAR data was successful, with many crowns having a 1 to 1 match with our manual segmentation, and high correlation among the crown size and AGB values (Supplementary material, Section S3). The reason for this success was that many agricultural trees were isolated and had crowns that were structurally distinct from the surrounding grassy vegetation.

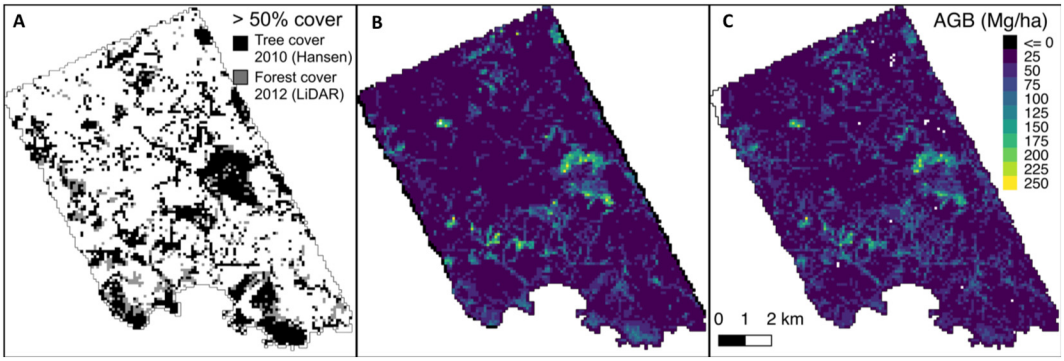

Fig. 7. Above ground biomass (AGB) estimates for 1 ha pixels of the 9280-hectare Azuero study site. A) Areas with > 50% cover from a 2010 global tree cover product (Hansen et al., 2013), and a 2012 forest cover product from LiDAR data used in this study. B) AGB estimates from the plot-based method of Asner et al., 2013. C) AGB estimates from the tree-based method developed in this study.

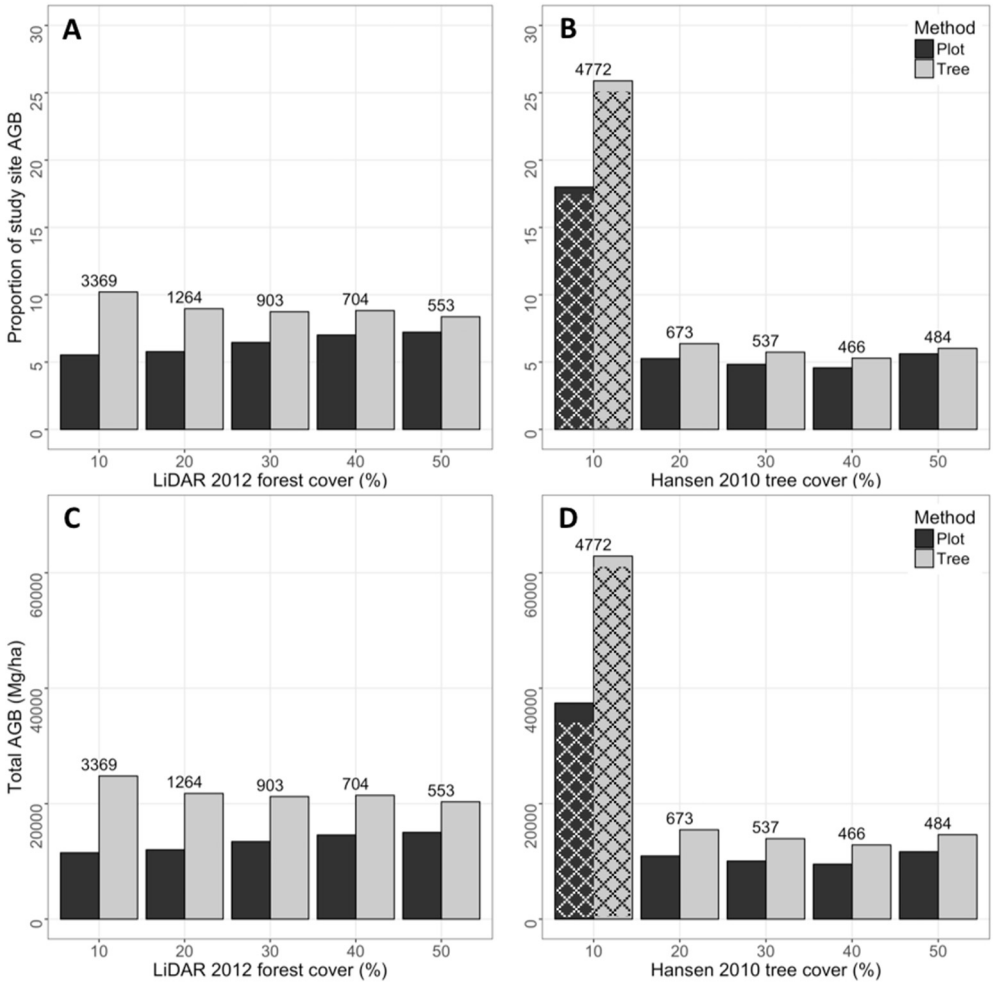

Fig. 8. Distribution of landscape above ground biomass (AGB) for tree-based (black bars, this study) and plot-based (grey bars, Asner et al., 2013) methods across 10% cover intervals. Two measures of canopy cover are shown; 2012 LiDAR forest cover from this study (panels A and C) and 2010 tree cover from a global tree cover product (panels B and D, Hansen et al., 2013). Labels above the bars are the hectares of the total landscape within each cover class. Hatched boxes in 10% bars for panels B and D show the proportion of AGB in areas with 0% tree cover in the Hansen dataset.

Crown dimensions from the crown segmentation for isolated trees have a strong correlation with dimensions from our manually segmented trees (after a 25% correction, Supplementary material, Section S2). In addition, the AGB estimates with our LiDAR model have little over or underestimation along the range of tree size. We note however that we needed to apply a 25% reduction in crown diameter derived from the segmentation even for isolated trees, indicating room for improvement for segmentation even in landscapes with relatively open tree canopy cover.

Crown segmentation was more challenging for trees in areas of intermediate and high canopy cover, where manually segmented crowns intersected many automatically segmented crowns, and the correlations between the size and AGB values were low (Supplementary material, Section S3). While trees in forests were not our primary target for this study, accurate estimates of their AGB are still important because they are part of the diverse tree cover landscape. Considering errors in the crown segmentation of forest trees, and the LiDAR AGB allometric model (Fig. 4D), we feel that trees in forests may be overestimated. Despite these patterns at the individual tree crown scale, when AGB estimates are scaled to 1-ha, the maximum AGB for the tree and plot-based approaches was similar, at 240 Mg/ha, and 254 Mg/ha, respectively (Fig. 8). Despite continued advancements in individual tree crown segmentation for closed canopy forests (Coomes et al., 2017; Ferraz et al., 2016), segmentation remains a primary challenge, especially for young forests composed of trees with small crowns.

4.2. Tree-based vs. plot-based estimates of AGB

Our study supports the development of tree-based approaches for estimating landscape biomass, particularly in agricultural landscapes, where plot-based methods do not account for heterogeneous tree cover that contributes to AGB. The differences among remote sensing methods that predict AGB (e.g. tree versus plot-based methods) influence conclusions about where AGB occurs on the landscape. Our results show that areas with 0–10% forest cover had tree-based estimates that were double those of the plot-based estimates (Fig. 8). Both tree and plot-based estimates are models of the landscape and therefore a simplification, but their differences present divergent views of where biomass is occurring, which has implications for monitoring, management, and policy decisions (Chazdon et al., 2016a).

There are advantages to plot-based methods, such as the simplicity, scalability to large landscapes, and ability to adjust the model to local conditions based on tree or carbon density (Asner and Mascaro, 2014; Colgan et al., 2013; Coomes et al., 2017). Plot-based methods provide continuous coverage, which is a crucial and important advancement from AGB estimates which focus only on areas defined as forest. Furthermore, the plot-based methods are calibrated and tested with field data, which also provides estimates of model uncertainty. Finally, although we used plot-based data with 1-ha resolution, there is an effort towards higher spatial resolution, which may detect finer gradients in tree cover. These are all important efforts that allow for the

quantification of biomass continuously over large areas, reducing bias of relying on statistical scaling of field-measured plots (Marvin et al., 2014).

However, this study, and others, highlight that plot-based methods may not accurately capture AGB in landscapes with a heterogeneous canopy, such as scattered trees in savanna ecosystems (Colgan et al., 2013) or forests with tall emergent trees and canopy gaps (Coomes et al., 2017). Using plot-based estimates is also not well-suited for agricultural landscapes if the purpose is to quantify national carbon stocks because there is a systematic under detection of AGB in areas with dispersed, low-density tree cover.

In the agricultural areas, one cause of the lower detection of AGB with plot-based methods may be lack of representation of areas with dispersed tree cover in field calibration plots. The field inventory data used in Asner et al. (2013) to establish the relationship between tree biomass and LiDAR data was focused on forested areas. Some plots were in regenerating forests, which is important for this landscape. However, there was no calibration in areas with active agriculture, an open canopy, and isolated trees. This means that the structure of these areas, and how it is detected in aggregated LiDAR data, is not accounted for in the modeling. The addition of field plots in active agricultural areas could aid in not only understanding the AGB storage and vegetation dynamics, but also in calibrating LiDAR data to the unique structure of agricultural landscapes.

As further evidence for the importance of measuring individual trees rather than aggregated plot-based data and methods, global tree cover in drylands using high resolution imagery produced an estimate of forest cover that was 43% higher than what had been produced with data that could not account for individual tree crowns (Bastin et al., 2017). While the plot-based estimates may be more simple and computationally less intensive to implement across large areas, their underrepresentation of tree cover and biomass should be taken into account, especially when used for carbon payment programs (Pelletier et al., 2011). We conclude that while the plot-based estimates may accurately capture the biomass in closed canopy forests, the methods are not accurately capturing the low density, heterogeneous, isolated tree cover that we know is common on agricultural landscapes in the tropics.

4.3. The importance of measuring trees outside forests

Trees outside forests are increasingly recognized as a critical provider of ecosystem services, including watershed protection, biodiversity conservation, and carbon storage and sequestration. As a result, efforts have been made to measure and monitor agricultural tree cover and consider it in management and policy decisions (Chazdon et al., 2016a). Our study supports these efforts by estimating AGB in an agricultural landscape using high resolution airborne LiDAR data and analysis methods that directly measure the presence and size of trees outside forests. We found that despite centuries of intensive agricultural land use, nearly 30% of landscape biomass (approximately 60,000 Mg) occurred in non-forested areas (non-forest as measured by a global product of tree cover from 30 m satellite data). The high contribution of these trees to landscape biomass highlights the need to accurately estimate and monitor, rather than ignore, trees in agricultural areas.

We emphasize that agricultural tree cover is not the same as a forest; a difference that is evident in forest definitions (Chazdon et al., 2016a), as well as forest cover products from remotely sensed data. We compared a global remote sensing product of tree cover (Hansen et al., 2013), with measurements of tree and forest cover from high resolution LiDAR data. The fine spatial resolution of the LiDAR data and segmentation algorithms can detect individual tree crowns in open areas better than in areas with a closed canopy (Fig. 3 A). The presence of these crowns is not represented in our product of forest cover, which deliberately excluded them, nor in the global tree cover product. The low cover estimates are apparent in areas where individual tree crowns have been detected in the LiDAR data (Fig. 3 B & C). Importantly, neither our forest cover dataset nor the global tree cover dataset captured the total tree cover on the landscape, which includes both closed canopy forested areas and low density, isolated trees outside forests (Fig. 3, Supplementary material, Section S4). While the global tree cover product (Hansen et al., 2013) is deliberately described as a tree cover product to avoid complications of forest definitions, we conclude it is measuring only large patches of continuous forest and missing the dispersed tree cover that exists on this agricultural landscape.

We present our results along a gradient of canopy cover to avoid imposing a crude forest and non-forest dichotomy on the landscape, which is a challenging task in landscapes such as the Azuero peninsula where there is both fine spatial scale heterogeneity and temporal variation. However, we want to highlight how using a global product of tree cover can be misleading and present much of the landscape as being void of ecological value. Rather than using the global tree cover product to define forested areas, we used it to identify areas that were classified as having zero to 10% cover and below, and are confident in concluding these areas would not be considered forest in any definition (Chazdon et al., 2016a). With this threshold, 52% of the study site would be considered non-forested in the global tree cover dataset, and 37% of the study site in our forest cover dataset (Supplementary material, Section S4). These non-forested areas have low AGB density relative to areas with higher cover (Figs. 5 & 7). However, because the non-forest areas dominate this study site, they contribute 10% of the total landscape AGB using our measurement of forest cover, and 26% of landscape AGB using the global tree cover dataset (Fig. 8). Therefore, if these non-forested areas were left out of global accounting of biomass or carbon stocks, nearly one third of AGB in this agricultural landscape would not be accounted for.

The high AGB estimates in non-forest areas found in our study and in global analyses (Zomer et al., 2016) highlights their ecological value in terms of carbon storage and sequestration. These findings support other work in quantifying the ecological and social value of trees in agricultural areas, and their continued protection (Chazdon et al., 2009). For example, field studies of this area, and similar areas in Costa Rica and Nicaragua, indicate tree cover is present in a diversity of forms, is utilized by wildlife, and has various ecological values for land managers (Harvey et al., 2006, 2011). With a recognition that these landscape features are important resources for people and the environment, more attention is being paid to them, including nationwide inventories (de Foresta et al., 2013), and global studies to understand the patterns and drivers of trees in agricultural areas (Zomer et al., 2014).

Accurate monitoring and quantification of biomass outside of forested areas is important in agricultural landscapes because of their potential to be a source or sink of carbon based on land management decisions. Agricultural tree cover could decline with the intensification of agriculture in the region as pastures are replaced with crops that require more machinery; a pathway that has been seen in other areas of Latin America (Graesser et al., 2015). There is also the potential for increased agricultural tree cover and greater carbon storage and sequestration in these tropical landscapes, which is occurring throughout our study site (Caughlin et al., 2016). These patterns could be driven by greater conservation activities in the region promoting silvopastoral systems or natural forest regeneration (Sandor and Chazdon, 2014).

5. Conclusion

Global climate change is a widely recognized problem being driven by a myriad of causes, one of which is believed to be the trend of tropical forest loss for the expansion of agriculture (Gibbs et al., 2010). To combat the loss of tropical forest cover, international programs are being developed to integrate tropical forests, and the goods and services they provide, into the global economy. However, the success of these programs requires accurate, reliable, and repeatable measurements of

landscape carbon stocks and sequestration rates (Gibbs et al., 2007).

While methods to estimate forest carbon stocks from remote sensing continue to be developed, we stress the need to develop and implement methods that can account for high variability in tree cover. Agricultural areas may have lower AGB density than forests, but they are a dominant global biome, and accurate quantification of biomass needs to be developed and implemented to keep agricultural areas in the dialogue of conservation policy and ecosystem management.

This study demonstrates that high resolution airborne data, in which individual trees can be resolved, may be a key to accurately assessing carbon stocks in agricultural landscapes. Furthermore, this study supports work to acknowledge and protect the ecological value of non-forest landscapes. We believe it is possible to understand patterns and dynamics of trees outside forests with remote sensing with the continued development of data products and methods that can capture these heterogeneous and dynamic landscapes.

Acknowledgements

The authors thank Diogenes Ibarra, Michelle Goodfellow, Lesely Candaleria, and Luis Mancilla, and members of the Azuero Earth Project, particularly Ruth Metzel and Jairo Batista-Bernal, for their support with field data collection. The remote sensing data collection, processing and analyses was supported by grants from the Grantham Foundation for the Protection of the Environment and William R. Hearst III. Funding for field data collection was provided by the Joshua C. Dickinson IV Fellowship and the Tinker Travel Fund through the University of Florida. The Carnegie Airborne Observatory has been made possible by the Avatar Alliance Foundation, Margaret A. Cargill Foundation, David and Lucile Packard Foundation, Gordon and Betty Moore Foundation, Grantham Foundation for the Protection of the Environment, W. M. Keck Foundation, John D. and Catherine T. MacArthur Foundation, Andrew Mellon Foundation, Mary Anne Nyburg Baker and G. Leonard Baker Jr, and William R. Hearst III. T. T. Caughlin was supported by National Science Foundation grant #1415297.

Appendix A. Supplementary material

Supplementary material for this article can be found online at https://doi.org/10.1016/j.rse.2018.09.009.

References

Aide, T.M., Clark, M.L., Grau, H.R., López-Carr, D., Levy, M.A., Redo, D., Bonilla-Moheno, M., Riner, G., Andrade-Núñez, M.J., Muñiz, M., 2013. Deforestation and reforestation of Latin America and the Caribbean (2001 − 2010). Biotropica 45, 262–271. https://doi.org/10.1111/j.1744-7429.2012.00908.x.

Asner, G.P., Mascaro, J., 2014. Mapping tropical forest carbon: calibrating plot estimates to a simple LiDAR metric. Remote Sens. Environ. 140, 614–624. https://doi.org/10.1016/j.rse.2013.09.023.

Asner, G.P., Knapp, D.E., Boardman, J., Green, R.O., Kennedy-Bowdoin, T., Eastwood, M., Martin, R.E., Anderson, C., Field, C.B., 2012. Carnegie Airborne Observatory-2: increasing science data dimensionality via high-fidelity multi-sensor fusion. Remote Sens. Environ. 124, 454–465. https://doi.org/10.1016/j.rse.2012.06.012.

Asner, G.P., Mascaro, J., Anderson, C., Knapp, D.E., Martin, R.E., Kennedy-Bowdoin, T., van Breugel, M., Davies, S., Hall, J.S., Muller-Landau, H.C., Potvin, C., Sousa, W., Wright, J., Bermingham, E., 2013. High-fidelity national carbon mapping for resource management and REDD+. Carbon Balance Manag. 8, 1–14. https://doi.org/10.1186/1750-0680-8-7.

Asner, G.P., Sousan, S., Knapp, D.E., Selmants, P.C., Martin, R.E., Hughes, R.F., Giardina, C.P., 2016. Rapid forest carbon assessments of oceanic islands: a case study of the Hawaiian archipelago. Carbon Balance Manag. 11 (1). https://doi.org/10.1186/s13021-015-0043-4.

Baccini, A., Goetz, S.J., Walker, W.S., Laporte, N.T., Sun, M., Sulla-Menashe, D., Hackler, J., Beck, P.S.A., Dubayah, R., Friedl, M.A., Samanta, S., Houghton, R.A., 2012. Estimated carbon dioxide emissions from tropical deforestation improved by carbon-density maps. Nat. Clim. Chang. 2, 182–185. https://doi.org/10.1038/nclimate1354.

Baskerville, G.L., 1972. Use of logarithmic regression in the estimation of plant biomass. Can. J. For. Res. 2, 49–53. https://doi.org/10.1139/x72-009.

Bastin, J.-F., Berrahmouni, N., Grainger, A., Maniatis, D., Mollicone, D., Moore, R., Patriarca, C., Picard, N., Sparrow, B., Abraham, E.M., Aloui, K., Atesoglu, A., Attore, F., Bassüllü, Ç., Bey, A., Garzuglia, M., García-Montero, L.G., Groot, N., Guerin, G., Laestadius, L., Lowe, A.J., Mamane, B., Marchi, G., Patterson, P., Rezende, M., Ricci, S., Salcedo, I., Diaz, A.S.-P., Stolle, F., Surappaeva, V., Castro, R., 2017. The extent of forest in dryland biomes. Science 356, 635–638 (80-.).

Caughlin, T.T., Rifai, S.W., Graves, S.J., Asner, G.P., Bohlman, S.A., 2016. Integrating LiDAR-derived tree height and Landsat satellite reflectance to estimate forest regrowth in a tropical agricultural landscape. Remote Sens. Ecol. Conserv. 2, 190–203. https://doi.org/10.1002/rse2.33.

Chave, J., Andalo, C., Brown, S., Cairns, M.A., Chambers, J.Q., Eamus, D., Fölster, H., Fromard, F., Higuchi, N., Kira, T., Lescure, J.-P., Nelson, B.W., Ogawa, H., Puig, H., Riéra, B., Yamakura, T., 2005. Tree allometry and improved estimation of carbon stocks and balance in tropical forests. Oecologia 145, 87–99. https://doi.org/10.1007/s00442-005-0100-x.

Chave, J., Muller-Landau, H.C., Baker, T.R., Easdale, T.A., ter Steege, H., Webb, C.O., 2006. Regional and phylogenetic variation of wood density across 2456 Neotropical tree species. Ecol. Appl. 16, 2356–2367.

Chave, J., Condit, R., Muller-Landau, H.C., Thomas, S.C., Ashton, P.S., Bunyavejchewin, S., Co, L.L., Dattaraja, H.S., Davies, S.J., Esufali, S., Ewango, C.E.N., Feeley, K.J., Foster, R.B., Gunatilleke, N., Gunatilleke, S., Hall, P., Hart, T.B., Hernández, C., Hubbell, S.P., Itoh, A., Kiratiprayoon, S., Lafrankie, J.V., Loo de Lao, S., Makana, J.-R., Noor, M.N.S., Kassim, A.R., Samper, C., Sukumar, R., Suresh, H.S., Tan, S., Thompson, J., Tongco, M.D.C., Valencia, R., Vallejo, M., Villa, G., Yamakura, T., Zimmerman, J.K., Losos, E.C., 2008. Assessing evidence for a pervasive alteration in tropical tree communities. PLoS Biol. 6, e45. https://doi.org/10.1371/journal.pbio.0060045.

Chave, J., Réjou-Méchain, M., Búrquez, A., Chidumayo, E., Colgan, M.S., Delitti, W.B.C., Duque, A., Eid, T., Fearnside, P.M., Goodman, R.C., Henry, M., Martínez-Yrízar, A., Mugasha, W.A., Muller-Landau, H.C., Mencuccini, M., Nelson, B.W., Ngomanda, A., Nogueira, E.M., Ortiz-Malavassi, E., Pélissier, R., Ploton, P., Ryan, C.M., Saldarriaga, J.G., Vieilledent, G., 2014. Improved allometric models to estimate the aboveground biomass of tropical trees. Glob. Chang. Biol. 20, 3177–3190. https://doi.org/10.1111/gcb.12629.

Chazdon, R.L., Harvey, C.A., Komar, O., Griffith, D.M., Ferguson, B.G., Martínez-Ramos, M., Morales, H., Nigh, R., Soto-Pinto, L., van Breugel, M., Philpott, S.M., 2009. Beyond reserves: a research agenda for conserving biodiversity in human-modified tropical landscapes. Biotropica 41, 142–153. https://doi.org/10.1111/j.1744-7429.2008.00471.x.

Chazdon, R.L., Brancalion, P.H.S., Laestadius, L., Bennett-Curry, A., Buckingham, K., Kumar, C., Moll-Rocek, J., Vieira, I.C.G., Wilson, S.J., 2016a. When is a forest a forest? Forest concepts and definitions in the era of forest and landscape restoration. Ambio 45, 538–550. https://doi.org/10.1007/s13280-016-0772-y.

Chazdon, R.L., Broadbent, E.N., Rozendaal, D.M.A., Bongers, F., Zambrano, A.M.A., Aide, T.M., Balvanera, P., Becknell, J.M., Boukili, V., Brancalion, P.H.S., Craven, D., Almeida-Cortez, J.S., Cabral, G.A.L., de Jong, B., Denslow, J.S., Dent, D.H., DeWalt, S.J., Dupuy, J.M., Durán, S.M., Espírito-Santo, M.M., Fandino, M.C., César, R.G., Hall, J.S., Hernández-Stefanoni, J.L., Jakovac, C.C., Junqueira, A.B., Kennard, D., Letcher, S.G., Lohbeck, M., Martínez-Ramos, M., Massoca, P., Meave, J.A., Mesquita, R., Mora, F., Muñoz, R., Muscarella, R., Nunes, Y.R.F., Ochoa-Gaona, S., Orihuela-Belmonte, E., Peña-Claros, M., Pérez-García, E.A., Piotto, D., Powers, J.S., Rodríguez-Velazquez, J., Romero-Pérez, I.E., Ruíz, J., Saldarriaga, J.G., Sanchez-Azofeifa, A., Schwartz, N.B., Steininger, M.K., Swenson, N.G., Uriarte, M., van Breugel, M., van der Wal, H., Veloso, M.D.M., Vester, H., Vieira, I.C.G., Bentos, T.V., Williamson, G.B., Poorter, L., 2016b. Carbon sequestration potential of second-growth forest regeneration in the Latin American tropics. Sci. Adv. 2.

Colgan, M.S., Asner, G.P., 2014. Coexistence and environmental filtering of species-specific biomass in an African savanna. Ecology 95, 1579–1590. https://doi.org/10.1890/13-1160.1.

Colgan, M.S., Asner, G.P., Swemmer, T., 2013. Harvesting tree biomass at the stand level to assess the accuracy of field and airborne biomass estimation in savannas. Ecol. Appl. 23, 1170–1184. https://doi.org/10.1890/12-0922.1.

Coomes, D.A., Dalponte, M., Jucker, T., Asner, G.P., Banin, L.F., Burslem, D.F.R.P., Lewis, S.L., Nilus, R., Phillips, O.L., Phua, M.-H., Qie, L., 2017. Area-based vs tree-centric approaches to mapping forest carbon in Southeast Asian forests from airborne laser scanning data. Remote Sens. Environ. 194, 77–88. https://doi.org/10.1016/j.rse.2017.03.017.

Dahlin, K.M., Asner, G.P., Field, C.B., 2012. Environmental filtering and land-use history drive patterns in biomass accumulation in a Mediterranean-type landscape. Ecol. Appl. 22, 104–118. https://doi.org/10.1890/11-1401.1.

Dalponte, M., Coomes, D.A., 2016. Tree-centric mapping of forest carbon density from airborne laser scanning and hyperspectral data. Methods Ecol. Evol. 7, 1236–1245. https://doi.org/10.1111/2041-210X.12575.

Dalponte, M., Reyes, F., Kandare, K., Gianelle, D., 2015. Delineation of individual tree crowns from ALS and hyperspectral data: a comparison among four methods. Eur. J. Remote Sens. 48, 365–382. https://doi.org/10.5721/EuJRS20154821.

Duncanson, L.I., Cook, B.D., Hurtt, G.C., Dubayah, R.O., 2014. An efficient, multi-layered crown delineation algorithm for mapping individual tree structure across multiple ecosystems. Remote Sens. Environ. 154, 378–386. https://doi.org/10.1016/j.rse.2013.07.044.

Duncanson, L., Rourke, O., Dubayah, R., 2015. Small sample sizes yield biased allometric equations in temperate forests. Sci. Rep. 5, 1–13. https://doi.org/10.1038/srep17153.

FAO, 2016. FAOSTAT database [WWW document]. URL. http://www.fao.org/faostat/en/#data/EL, Accessed date: 28 November 2017.

Ferraz, A., Saatchi, S., Mallet, C., Meyer, V., 2016. Lidar detection of individual tree size in tropical forests. Remote Sens. Environ. 183, 318–333. https://doi.org/10.1016/j.rse.2016.05.028.

de Foresta, H., Somarriba, E., Temu, A., Boulanger, D., Feuilly, H., Gauthier, M., 2013. Towards the Assessment of Trees Outside Forests (No. 183), Forest Resources Assessment. Rome.

Gibbs, H.K., Brown, S., Niles, J.O., Foley, J. a, 2007. Monitoring and estimating tropical forest carbon stocks: making REDD a reality. Environ. Res. Lett. 2, 045023. https://doi.org/10.1088/1748-9326/2/4/045023.

Gibbs, H.K., Ruesch, A.S., Achard, F., Clayton, M.K., Holmgren, P., Ramankutty, N., Foley, J.A., 2010. Tropical forests were the primary sources of new agricultural land in the 1980s and 1990s. Proc. Natl. Acad. Sci. U. S. A. 107, 16732–16737. https://doi.org/10.1073/pnas.0910275107.

Girardin, C.A.J., Malhi, Y., Aragao, L.E.O.C., Mamani, M., Huaraca Huasco, W., Durand, L., Feeley, K.J., Rapp, J., Silva-Espejo, J.E., Silman, M., Salinas, N., Whittaker, R.J., 2010. Net primary productivity allocation and cycling of carbon along a tropical forest elevational transect in the Peruvian Andes. Glob. Chang. Biol. 16, 3176–3192. https://doi.org/10.1111/j.1365-2486.2010.02235.x.

Graesser, J., Aide, T.M., Grau, H.R., Ramankutty, N., 2015. Cropland/pastureland dynamics and the slowdown of deforestation in Latin America. Environ. Res. Lett. 10, 034017. https://doi.org/10.1088/1748-9326/10/3/034017.

Graves, S., Asner, G., Martin, R., Anderson, C., Colgan, M., Kalantari, L., Bohlman, S., 2016. Tree species abundance predictions in a tropical agricultural landscape with a supervised classification model and imbalanced data. Remote Sens. 8, 161. https://doi.org/10.3390/rs8020161.

Griscom, H.P., Connelly, A.B., Ashton, M.S., Wishnie, M.H., Deago, J., 2011. The structure and composition of a tropical dry forest landscape after land clearance; Azuero peninsula, Panama. J. Sustain. For. 30, 37–41.

Hansen, M.C., Potapov, P.V., Moore, R., Hancher, M., Turubanova, S.A., Tyukavina, A., Thau, D., Stehman, S.V., Goetz, S.J., Loveland, T.R., Kommareddy, A., Egorov, A., Chini, L., Justice, C.O., Townshend, J.R.G., 2013. High-resolution global maps of 21st-century forest cover change. Science 342, 850–853 (80-.).

Harvey, C.A., Haber, W.A., 1999. Remnant trees and the conservation of biodiversity in Costa Rican pastures. Agrofor. Syst. 44, 37–68. https://doi.org/10.1023/A:1006122211692.

Harvey, C.A., Villanueva, C., Villacís, J., Chacón, M., Muñoz, D., López, M., Ibrahim, M., Gómez, R., Taylor, R., Martinez, J., Navas, A., Saenz, J., Sánchez, D., Medina, A., Vilchez, S., Hernández, B., Perez, A., Ruiz, F., López, F., Lang, I., Sinclair, F.L., 2005. Contribution of live fences to the ecological integrity of agricultural landscapes. Agric. Ecosyst. Environ. 111, 200–230. https://doi.org/10.1016/j.agee.2005.06.011.

Harvey, C.A., Medina, A., Sánchez, D.M., Vilchez, S., Hernández, B., Saenz, J.C., Maes, J.M., Casanoves, F., Sinclair, F.L., 2006. Patterns of animal diversity in different forms of tree cover in agricultural landscapes. Ecol. Appl. 16, 1986–1999.

Harvey, C.A., Villanueva, C., Esquivel, H., Gómez, R., Ibrahim, M., Lopez, M., Martinez, J., Muñoz, D., Restrepo, C., Saénz, J.C., Villacís, J., Sinclair, F.L., 2011. Conservation value of dispersed tree cover threatened by pasture management. For. Ecol. Manag. 261, 1664–1674. https://doi.org/10.1016/j.foreco.2010.11.004.

Heckadon Moreno, S., 2009. De selvas a potreros: la colonización santeña en Panamá, 1850–1980. Exedra Books.

Henry, H.A.L., Aarssen, L.W., 1999. The interpretation of stem diameter-height allometry in trees: biomechanical constraints, neighbour effects, or biased regressions? Ecol. Lett. 2, 89–97. https://doi.org/10.1046/j.1461-0248.1999.22054.x.

Holbrook, N.M., Putz, F.E., 1989. Influence of neighbors on tree form: effects of lateral shade and prevention of sway on the allometry of *Liquidambar styraciflua* (sweet gum). Am. J. Bot. 76, 1740. https://doi.org/10.2307/2444473.

Jucker, T., Caspersen, J., Chave, J., Antin, C., Barbier, N., Bongers, F., Dalponte, M., van Ewijk, K.Y., Forrester, D.I., Haeni, M., Higgins, S.I., Holdaway, R.J., Iida, Y., Lorimer, C., Marshall, P.L., Momo, S., Moncrieff, G.R., Ploton, P., Poorter, L., Rahman, K.A., Schlund, M., Sonké, B., Sterck, F.J., Trugman, A.T., Usoltsev, V.A., Vanderwel, M.C., Waldner, P., Wedeux, B.M.M., Wirth, C., Wöll, H., Woods, M., Xiang, W., Zimmermann, N.E., Coomes, D.A., 2016. Allometric equations for integrating remote sensing imagery into forest monitoring programmes. Glob. Chang. Biol. 1–14. https://doi.org/10.1111/gcb.13388.

Kuyah, S., Dietz, J., Muthuri, C., Jamnadass, R., Mwangi, P., Coe, R., Neufeldt, H., 2012. Allometric equations for estimating biomass in agricultural landscapes: I. aboveground biomass. Agric. Ecosyst. Environ. 158, 216–224.

Laurance, W.F., Lovejoy, T.E., Vasconcelos, H.L., Bruna, E.M., Didham, R.K., Stouffer, P.C., Gascon, C., Bierregaard, R.O., Laurance, S.G., Sampaio, E., 2002. Ecosystem decay of Amazonian forest fragments: a 22-year investigation. Conserv. Biol. 16, 605–618. https://doi.org/10.1046/j.1523-1739.2002.01025.x.

León, M.C., Harvey, C.A., 2006. Live fences and landscape connectivity in a neotropical agricultural landscape. Agrofor. Syst. 68, 15–26. https://doi.org/10.1007/s10457-005-5831-5.

Lines, E.R., Zavala, M.A., Purves, D.W., Coomes, D.A., 2012. Predictable changes in aboveground allometry of trees along gradients of temperature, aridity and competition. Glob. Ecol. Biogeogr. 21, 1017–1028. https://doi.org/10.1111/j.1466-8238.2011.00746.x.

Marvin, D.C., Asner, G.P., Knapp, D.E., Anderson, C.B., Martin, R.E., Sinca, F., Tupayachi, R., 2014. Amazonian landscapes and the bias in field studies of forest structure and biomass. Proc. Natl. Acad. Sci. 111, E5224–E5232. https://doi.org/10.1073/pnas.1412999111.

Medina, A., Harvey, C.A., Sánchez Merlo, D., Vilchez, S., Hernández, B., 2007. Bat diversity and movement in an agricultural landscape in Matiguás, Nicaragua. Biotropica 39, 120–128.

Metzel, R., Montagnini, F., 2014. From farm to forest: factors associated with protecting and planting trees in a Panamanian agricultural landscape. Bois Forets des Trop. 322, 3–15.

Olson, D.M., Dinerstein, E., Wikramanayake, E.D., Burgess, N.D., Powell, G.V.N., Underwood, E.C., D'amico, J.A., Itoua, I., Strand, H.E., Morrison, J.C., Loucks, C.J., Allnutt, T.F., Ricketts, T.H., Kura, Y., Lamoreux, J.F., Wettengel, W.W., Hedao, P., Kassem, K.R., 2001. Terrestrial ecoregions of the world: a new map of life on earth. Bioscience 51, 933–938. https://doi.org/10.1641/0006-3568(2001)051[0933:TEOTWA]2.0.CO;2.

Pan, Y., Birdsey, R.A., Fang, J., Houghton, R., Kauppi, P.E., Kurz, W.A., Phillips, O.L., Shvidenko, A., Lewis, S.L., Canadell, J.G., Ciais, P., Jackson, R.B., Pacala, S.W., McGuire, A.D., Piao, S., Rautiainen, A., Sitch, S., Hayes, D., 2011. A large and persistent carbon sink in the world's forests. Science 333, 988–993. https://doi.org/10.1126/science.1201609.

Park, A., van Breugel, M., Ashton, M.S., Wishnie, M., Mariscal, E., Deago, J., Ibarra, D., Cedeño, N., Hall, J.S., 2010. Local and regional environmental variation influences the growth of tropical trees in selection trials in the Republic of Panama. For. Ecol. Manag. 260, 12–21. https://doi.org/10.1016/j.foreco.2010.03.021.

Pelletier, J., Ramankutty, N., Potvin, C., 2011. Diagnosing the uncertainty and detectability of emission reductions for REDD+ under current capabilities: an example for Panama. Environ. Res. Lett. 6, 024005. https://doi.org/10.1088/1748-9326/6/2/024005.

Plieninger, T., 2012. Monitoring directions and rates of change in trees outside forests through multitemporal analysis of map sequences. Appl. Geogr. 32, 566–576. https://doi.org/10.1016/j.apgeog.2011.06.015.

Prevedello, J.A., Almeida-Gomes, M., Lindenmayer, D.B., 2017. The importance of scattered trees for biodiversity conservation: a global meta-analysis. J. Appl. Ecol. https://doi.org/10.1111/1365-2664.12943.

Sandor, M.E., Chazdon, R.L., 2014. Remnant trees affect species composition but not structure of tropical second-growth forest. PLoS One 9, e83284. https://doi.org/10.1371/journal.pone.0083284.

Slocum, M.G., Horvitz, C.C., 2000. Seed arrival under different genera of trees in a neotropical pasture. Plant Ecol. 149, 51–62. https://doi.org/10.1023/A:1009892821864.

Zahawi, R.A., Holl, K.D., Cole, R.J., Reid, J.L., 2013. Testing applied nucleation as a strategy to facilitate tropical forest recovery. J. Appl. Ecol. 50, 88–96. https://doi.org/10.1111/1365-2664.12014.

Zhen, Z., Quackenbush, L., Zhang, L., 2016. Trends in automatic individual tree crown detection and delineation—evolution of LiDAR data. Remote Sens. 8, 333. https://doi.org/10.3390/rs8040333.

Zomer, R.J., Trabucco, A., Coe, R., Place, F., van Noordwijk, M., Xu, J., 2014. Trees on Farms: An Update and Reanalysis of Agroforestry's Global Extent and Socio-ecological Characteristics (No. 179). Bagor. https://doi.org/10.5716/WP14064.PDF.

Zomer, R.J., Neufeldt, H., Xu, J., Ahrends, A., Bossio, D., Trabucco, A., van Noordwijk, M., Wang, M., 2016. Global tree cover and biomass carbon on agricultural land: the contribution of agroforestry to global and national carbon budgets. Sci. Rep. 6 (29987). https://doi.org/10.1038/srep29987.